# How to estimate scavenger fish abundance using baited camera data

**K. D. Farnsworth**[1,*]**, U. H. Thygesen**[2]**, S. Ditlevsen**[3]**, N. J. King**[4]

[1]**School of Biological Science, Queens University Belfast, 97 Lisburn Road, Belfast BT9 7BL, UK**
[2]**Danmarks Fiskeriundersøgelser Afd. for Havfiskeri, Charlottenlund Slot, 2920 Charlottenlund, Denmark**
[3]**Biostatistisk Afdeling, Københavns Universitet, Øster Farimagsgade 5, Opgang B, Postboks 2099, 1014 Copenhagen, Denmark**
[4]**Oceanlab, University of Aberdeen, Main Street, Newburgh, Aberdeenshire AB41 6AA, UK**

ABSTRACT: Baited cameras are often used for abundance estimation wherever alternative techniques are precluded, e.g. in abyssal systems and areas such as reefs. This method has thus far used models of the arrival process that are deterministic and, therefore, permit no estimate of precision. Furthermore, errors due to multiple counting of fish and missing those not seen by the camera have restricted the technique to using only the time of first arrival, leaving a lot of data redundant. Here, we reformulate the arrival process using a stochastic model, which allows the precision of abundance estimates to be quantified. Assuming a non-gregarious, cross-current-scavenging fish, we show that prediction of abundance from first arrival time is extremely uncertain. Using example data, we show that simple regression-based prediction from the initial (rising) slope of numbers at the bait gives good precision, accepting certain assumptions. The most precise abundance estimates were obtained by including the declining phase of the time series, using a simple model of departures, and taking account of scavengers beyond the camera's view, using a hidden Markov model.

KEY WORDS: Deep sea · *Coryphaenoides* · Lander · Hidden Markov model · Population · Wildlife census

## INTRODUCTION

Estimates of organism abundance are fundamental for marine ecology, but particularly difficult in many circumstances that preclude the intensive use of trawl sampling, or acoustic survey, e.g. abyssal systems and areas such as reefs, where trawls cannot run or would damage the sea floor unacceptably. Priede & Merrett (1998) recommended the deployment of autonomous lander platforms equipped with bait and camera systems as a relatively low-cost and low-impact alternative. In early work, Priede et al. (1990) successfully fitted an empirical curve to the time series of scavenger numbers present at a bait on the sea floor; this was later used to estimate (the assumed constant) staying time at bait (Henriques et al. 2002). Additionally, Priede & Merrett (1996) found an empirical relationship $\lambda \propto \tau_1^{-2}$, between the time to first fish arrival, $\tau_1$, and environmental fish density, $\lambda$, determined independently by trawling. Following these dis-

coveries, interpretation of statistics other than first arrival time had not succeeded in predicting organism abundance (Priede & Merrett 1998), and thus has not been considered further.

More recent emphasis has been placed on using mechanistic models of the arrival process (Priede & Bagley 2000, Bailey & Priede 2002, Collins et al. 2002). These models make assumptions about foraging behaviour and the spatial distribution of scavengers, as well as the prevailing current, swimming speeds and odour plume development (linear extension and diffusive spread). The models fall into 2 main categories—those assuming actively searching foragers (usually fish) and those, following earlier work by Sainte-Marie & Hargrave (1987), assuming that scavengers passively wait for signs of food arriving on a spreading plume. In reality there is a continuum between these 2 extremes depending on the speed of searching relative to passive diffusion. For passive scavengers, a descrip-

tion of the plume is most important, but the crux of models with active scavengers is accurate representation of their search strategy in relation to the current (Bailey & Priede 2002). There is good evidence that swimming in an approximately orthogonal direction to the current is optimal (Dusenbery 1989, Vabo et al. 2004) and is commonly displayed by scavengers (Priede et al. 1991, Bailey & Priede 2002). Consequently, Bailey & Priede (2002) derived a deterministic model of arrival rate for cross-current scavengers and showed it was able to predict first arrival times, though they found this measure was relatively insensitive to abundance above about 100 ind. km$^{-2}$.

Biologists with time series data collected from baited camera deployments are still faced with the question of how to make the most effective and justifiable use of the data in estimating organism abundance. This is not by any means a simple question, as it depends on arrival and departure statistics, scavenger behaviour throughout the feeding cycle, and the limitations of the equipment used. The aim of the present work was to provide guidelines for estimating abundance from baited camera data, specifically for fish scavengers that actively search, rather than sit and wait, for odour plumes. We shall first build a conceptual model of the processes determining numbers of fish seen at the bait. Then we will assess 3 indirect measures of abundance using these counts, in order of increasing use of the data. Each measure will be demonstrated using example data taken from observations of *Coryphaenoides armatus* in the Nazaré Canyon, west of Portugal (King 2006). The important attributes of each method will be illustrated, showing its strengths and weaknesses; in particular, we shall show how the precision of the techniques increases as more information is used. The ecological time scale to which our analysis applies is that of the time series of camera observations in a single deployment.

## CONCEPTUAL MODEL

The number of fish attending the bait results from a balance between arrivals and departures (Sainte-Marie & Hargrave 1987). The arrival rate depends on the number that are attracted to the bait, which is determined by the abundance of scavenger fish able to detect the plume, and the proportion of them that respond by swimming to the bait. We note here that the presence of competitors and predators near the bait can affect the bait's attractiveness (see Lapointe & Saint-Marie 1992), but such effects are separate from the main estimation problem and we do not deal with them further. Hence, we assume that fish that can detect the bait will attend it. Even with this assumption, assessing counts at the bait is complicated by the fact that fish

may arrive at the bait, circle it, perhaps exiting the camera view and may repeatedly return to the bait before finally leaving the area around the bait (bait zone) altogether (Collins et al. 1999). These behaviours potentially undermine efforts to estimate abundance (Yau et al. 2001), but a common response has been to average observed numbers of fish over several replications of bait deployment; for example, Priede et al. (1994) took the maximum mean number observed per block of 15 image frames as a best estimate of true numbers. We hope to improve on such heuristics. To facilitate reference to calculations, the symbols used and their ranges have been collated in Table 1.

Arrival rate is stochastically related to population density. Departure rate depends on the number of fish present at the bait and the fish behaviour (determining residence time), and the observable fraction depends on both movements local to the bait and the visual scope of the camera. These processes are brought together in the conceptual model (Fig. 1), in which $n(t)$ is the expected (mean) number of fish that have been attracted to the bait, but are not in the view of the camera and $m(t)$ is the expected number that are photographed. Thus, in our model, fish are attracted to the bait zone at a stochastic rate $\rho_a(t)$ and switch between this state and the 'in camera' state at rate $\zeta$, finally departing the bait zone at a stochastic rate of $\rho_d(t)$ (Fig. 1).

We make a simplifying assumption that the switching rate between in-camera and out-of-camera states is symmetrical (individual fish in the region are equally likely to become apparent as become obscure) and is therefore $\zeta[n(t) - m(t)]$. Conservation of numbers (fish are neither created nor destroyed here) ensures that after a time $T$:

$$n(T) + m(T) = \int_0^T [\rho_a(\lambda,t) - \rho_d(t)]\mathrm{d}t \qquad (1)$$

and inspection of flow rates yields the following pair of differential equations:

$$\frac{\mathrm{d}n(t)}{\mathrm{d}t} = \rho_a(\lambda,t) + \zeta m(t) - (\rho_d + \zeta)n(t) \qquad (2)$$

$$\frac{\mathrm{d}m(t)}{\mathrm{d}t} = \zeta[n(t) - m(t)] \qquad (3)$$

The resulting time series of numbers at the bait has the following general features: a delay phase before the first arrival, a growth phase during which the arrival rate exceeds the departure rate, and a decay phase in which departures exceed arrivals and, hence, a maximum in numbers when the arrival rate equals the departure rate (these features are shown in Bailey & Priede 2002, their Fig. 3). Superimposed on this gross pattern, the time series shows random rises and falls due to movements in and out of the field of view, as well as the stochasticity of arrival and departure processes. The above equations serve to explain the processes involved, but they are con-

Table 1. Symbols and their definitions, the quantities in the model, the dimensions, their range and the values used here

| | Description | Units | Range | Typical |
|---|---|---|---|---|
| $A(t)$ | Area from which fish will reach the bait in time $t$ | $m^2$ | $A \geq 0$ | – |
| $\alpha(t)$ | A constant gathering speed terms in the stochastic model | $m^2\,s^{-2}$ | $\alpha > 0$ | – |
| $D$ | Diffusion coefficient of fish | $l^2\,s^{-1}$ | $D > 0$ | $0.01^c$ |
| $J$ | Flux of fish | fish $l^{-2}\,s^{-1}$ | $J > 0$ | – |
| $\lambda$ | Mean density of scavengers in the environment | fish $m^{-2}$ | $\lambda \geq 0$ | $10^{-4}$ |
| $\Lambda$ | Constant in an empirical model of number of fish observed | fish $s^{-\varphi}$ | $\Lambda \geq 0$ | – |
| $\gamma$ | Shape parameter of the Weibull distribution[a] | – | $\gamma > 0$ | – |
| $\beta$ | Scale parameter of the Weibull distribution[b] | – | $\beta > 0$ | – |
| $\varphi$ | Non-linear regression scaling constant | – | $\varphi > 0$ | $1 < \varphi < 3$ |
| $q$ | Quintile of a statistical distribution | – | – | – |
| $m(t)$ | Expected number of fish in camera view | fish | $m(t) \geq 0$ | – |
| m($t$) | Observed number of fish in camera view | fish | m($t$) $\geq 0$ | – |
| $n(t)$ | Expected number of fish hidden from the camera | fish | $n(t) \geq 0$ | – |
| n($t$) | Hypothetically 'observed' number of hidden fish | fish | n($t$) $\geq 0$ | – |
| $N(t)$ | Expected number of fish arrived after time $t$ | fish | $N(t) \geq 0$ | – |
| $\mu$ | Expected rate of reorientation in foraging fish | $s^{-1}$ | $\mu \geq 0$ | $10^{-3}$ |
| $p$ | Observable fraction of fish in the bait zone | – | $0 < p < 1$ | – |
| $\rho_a(t)$ | Rate of arrival of fish at the bait zone | $s^{-1}$ | $\rho_a > 0$ | – |
| $\rho_d(t)$ | Rate of departure of fish at the bait zone | $s^{-1}$ | $\rho_d \geq 0$ | – |
| $T$ | A finite time after deployment of the baited camera | s | $T > 0$ | – |
| $\tau_1$ | Time of arrival of first fish | s | $\tau_1 > 0$ | $10^3$ |
| $\tau^\bullet$ | Time when observed number of fish becomes maximum | s | $\tau^\bullet > 0$ | $10^3$ |
| $u$ | Speed of the current | $m\,s^{-1}$ | $u > 0$ | 0.05 |
| $v$ | Fish swimming speed against the current (upstream) | $m\,s^{-1}$ | $v > 0$ | 0.05 |
| $w$ | Fish searching speed perpendicular to the current | $m\,s^{-1}$ | $w > 0$ | 0.05 |
| $x(t)$ | Total number of fish in the bait zone | fish | $x(t) > 0$ | – |
| $\bar{z}$ | Estimate of parameter controlling rate of change of $\rho_d(t)$ | fish $s^{-2}$ | – | – |
| $\zeta$ | Switching rate in and out of camera view | $s^{-1}$ | $\zeta \geq 0$ | – |

[a]As $\beta$ increases, the PDF of the distribution lowers and spreads (see Johnson et al. 1994)

[b]As $\gamma$ increases, the PDF of the distribution becomes more symmetrical (Johnson et al. 1994)

[c]Unsupported by published data



Fig. 1. Poisson processes of the 'bait zone' governing the number of fish seen by the camera at time $t$: $\rho_a$ is the true arrival rate, $\zeta$ is the rate of switching in and out of view of the camera and $\rho_d$ is the true departure rate

tinuous approximations. Next, we develop stochastic models that explicitly count individuals because the numbers involved are small.

## MODELS OF FISH ARRIVAL RATES

Two models will be considered: the first assumes that fish swim with constant velocity across the current (geometric model) and the second allows for random direction switching (diffusion model). The models give different predictions on how the number of arriving fish increases with time; empirical estimation of this rate will later be used to select the model which best fits a time series of fish arrivals.

**Geometric model of fish arrivals.** We assume a constant velocity water current, with fish searching orthogonally (cross-current) for odour plumes. Given that fish searching speed is likely to be much greater than the odour diffusion rate (see Yen et al. 1998, Webster & Weissburg 2001), diffusive spreading has a negligible effect on arrival times. This greatly simplifies the problem by reducing the plume to a 1-dimensional target extending in space at the same rate (and in the same direction) as the current.

We use a coordinate system with the bait as the origin, with the positive $y$-direction defined by the current direction as it flows with constant speed $u$. Fish move perpendicularly to the current (the $x$-axis) at a constant speed $w$; on average, half of them move in the positive $x$-direction and the other half move in the negative $x$-direction. Once they encounter the plume, they swim up it at a speed $v$ over the substrate by swimming faster than the opposing current. We also assume that fish act independently of one another, are equivalent in all respects, swim with constant velocity (except where stated) and that there is only 1 attractant (these fish cannot be distracted).
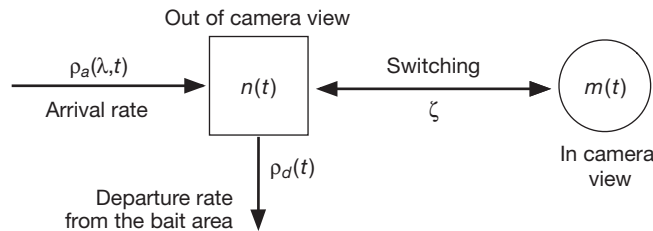
At time 0 the bait is placed at coordinates $(0,0)$. At time $t, \in [0,T]$, the bait can be detected in the set $\{(x,y):$ $x = 0,\ 0 \le y \le ut\}$—this defines the plume as a line extending in the $y$-direction at a constant rate $u$. Since fish can swim both left and right across the current, we assume half of them do each, and, since the system is symmetrical about the plume's axis, we can simplify by considering only 1 side (halving the swept area), and assuming 1 swimming direction (doubling the fish interceptions), cancelling factors of 2, this is equivalent to the complete system. A fish starting at position $(x,y)$, $x \ge 0,\ y \ge 0$, swimming to the left (direction $-x$), can reach the plume at time $x/w$ and the bait at time $x/w + y/v$. Thus, for the fish to arrive at the bait, the following must be true: $x/w + y/v \le T$ or $y \le vT - vx/w$. Since the fish crosses the line $x = 0$ at time $x/w$, it will only detect the bait plume if $x/w \ge y/u$ or $y \le ux/w$. Therefore, between time 0 and time $T$ the fish arriving at the bait must have been in the following triangular region at time 0:

$$\{(x,y): x \ge 0, y \ge 0, y \le vT - vx/w, y \le ux/w\}$$

which we call the 'swept area' $A(T)$. Fig. 2 illustrates the geometry of this argument, and Fig. 3 shows how the 3 boundaries defining the swept area are used to calculate its size for a given value of $T$:

$$A(T) = \frac{1}{2}\frac{uvT}{(u+v)}wT = \frac{uvwT^2}{2(u+v)} = \alpha T^2 \tag{4}$$

defining a constant $\alpha$.

If the initial configuration of fish in the plane is a Poisson process with intensity $\lambda$ (meaning a random 2-dimensional distribution of mean density $\lambda$), then the
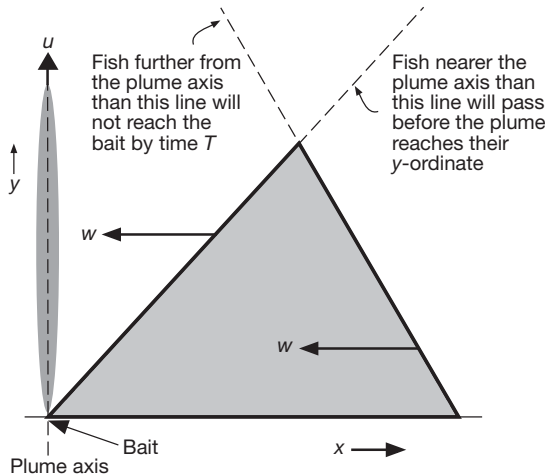


Fig. 2. Explanation of 'swept area' $A(T)$ for fish swimming right to left searching for a plume. Those within the shaded triangle will meet the plume and swim to the bait all within time $T$. If they are too near the plume axis, they will swim past it before the plume extends to their $y$-ordinate; if they are too far from the plume axis, they will not reach it in time to have swum to the bait before the deadline of $T$ seconds
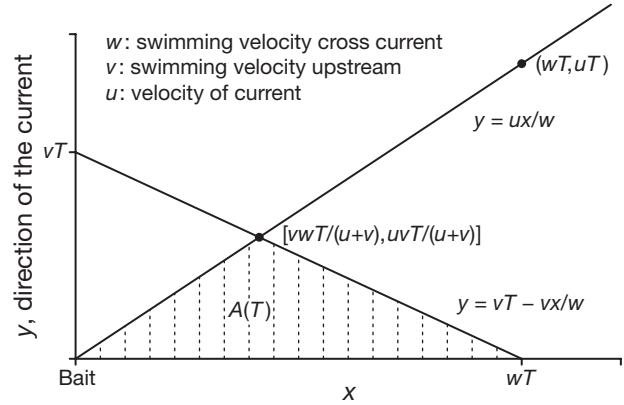


Fig. 3. Calculation of swept area: fish swim past the plume axis if $y > ux/w$ and fail to reach the bait in time $T$ if $y > vT - vx/w$. These 2 inequalities, along with the positive $y$ rule: $y > 0$, define the swept area triangle—the solutions to their corresponding equations give us the triangle's dimensions, and hence, the area

number of fish expected to have arrived at time $t$ is Poisson distributed with an expected value (denoted by $\mathbf{E}[N_t]$:

$$\mathbf{E}[N_t] = \lambda\alpha t^2 \tag{5}$$

Correspondingly, the time of arrival of each fish, marked on a time line, is a Poisson process of intensity:

$$\lambda\frac{\mathrm{d}A}{\mathrm{d}t} \tag{6}$$

Assuming continuous linear growth of the plume, this intensity will grow linearly in time. Ultimately, the plume will be diluted below the detection threshold of searching fish, from this point the quadratic scaling would be replaced by a linear extrapolation giving a constant arrival rate. However, for simplicity we assume that at least until the first fish arrives, the plume is not truncated. Since Lokkeborg et al. (1995) found sablefish *Anoplopoma fimbria* to be able to detect food odour plumes over 1000s of metres and since dispersion is likely to be small over this scale (Zimmer-Faust et al. 1995), we expect the assumption to be reasonable over the time scale of several 10s of hours, which is typical of bait deployments.

**Diffusion model of fish arrivals.** Relaxing the assumption that fish swim with constant velocity forever, we allow them to occasionally turn in the opposite direction during cross-current foraging. We call this behaviour 'reorientation' and assume that it occurs at independently random times, thus constituting a Poisson process for the individual fish. We denote the expected rate of reorientation as $\mu$ and assume it to be constant.

When the time since deployment of the bait is much shorter than $1/\mu$, we do not need to take reorientations into account, but, when it is much larger, the movement of the fish can be approximated with Brownian

motion (Okubo 1980), characterised by an equivalent diffusivity, $D = w^2\mu$ (since with orthogonal searching, this is effectively a 1-dimensional system).

In this diffusive model, we can estimate the flux of fish to the bait by first considering the diffusion problem $\dot{C} = D\nabla^2 C$ with the absorbing boundary $C(0,t) = 0$, far field $C(\infty,t) = C_\infty$ and initial condition $C(x,0) = C_\infty$. In this partial differential equation system, used to define diffusion, $C$ represents the concentration of particles (in our case fish) and $D$ can be interpreted as the rate at which they spread from a point ($\nabla$ is the Del operator—representing multi-dimensional differentiation). The solution of this system is well known (e.g. Okubo 1980):

$$C(x,t) = C_\infty \text{erf}[x/(2\sqrt{Dt})] \qquad (7)$$

(in which erf[$z$] is the 'error function', familiar in mathematical physics—it is twice the integral of the Gaussian distribution with 0 mean and variance $\frac{1}{2}$, from zero to $z$). From the solution, we find the flux to the origin from the positive half axis:

$$J(t) = D\nabla C(0,t) = C_\infty \sqrt{D/\pi t} \qquad (8)$$

which again follows textbook mathematics.
Now we apply this basic result to the present problem: for a fish to arrive at the bait at time $t$, it must have had an initial $y$-coordinate such that $y/u + y/v \leq t$, since first the plume must reach distance $y$, and the fish needs time to reach the bait after encountering the plume. It must have arrived at the plume a time interval $t - y/u - y/v$ after the plume reached an extension of $y$. Integrating over all such $y$, we find the instantaneous flux of fish to the bait at time $t$:

$$\int_0^{t/(1/u+1/v)} \lambda 2\sqrt{D/\pi} \frac{1}{\sqrt{t - y/u - y/v}} \, dy = \sqrt{t}\frac{vu}{v+u} 4\lambda\sqrt{D/\pi} \quad (9)$$

This shows that the flux to the bait scales with $\sqrt{t}$, which is the expected scaling for a diffusive process. Eq. (9) can be interpreted in terms of a 'swept area', analogous to the $A(t)$ we had before. It states that the expected number of fish arriving at the bait no later than $t$ is the expected number of fish contained within a parabolic region defined by the speed constants $(v,u,w)$ and $D$. The area of this parabolic region scales as $t\sqrt{t}$.

**Distribution of first arrival times.** First arrival times are the standard measure for estimating abundance using deterministic models (following Priede & Bagley 2000). Here, we derive the stochastic equivalent and, from this, determine the theoretical precision of abundance estimates based on first arrival time, assuming that the camera accurately records the true arrival time of the first fish. The following analysis applies for both the geometric and diffusion models, and more generally.

We use the stochastic variable $n(t)$ to describe the observed number of fish at time $t$, which is Poisson distributed with expectation $\mathbf{E}[n(t)] = n(t) = \lambda A(t)$, so $n(t)$ denotes a sort of 'average' number we expect to see at time $t$. Let $\tau_1$ be the time of arrival of the first fish. This will occur after time $t$ only if $n(t) = 0$, and from the definition of the Poisson distribution the probability of this is:

$$\mathbf{P}(\tau_1 > t) = \mathbf{P}[n(t) = 0] = \exp[-\lambda A(t)] \qquad (10)$$

We find the probability density function (PDF) of $\tau_1$ by differentiating with respect to time:

$$P(\tau_1 \in [t, t + dt])/dt = \lambda(dA/dt)\exp[-\lambda A(t)] \qquad (11)$$

If we now let $A(t) = \alpha t^\gamma$ (allowing for the geometric, diffusion, and more general models of arrivals), then Eq. (11) gives the PDF:

$$P(\tau_1) = \gamma\alpha\lambda\tau_1^{\gamma-1}\exp(-\lambda\alpha\tau_1^\gamma) \qquad (12)$$

We recognise this density of $\tau_1$ to be that of a Weibull distribution (which is the subject of Chapter 21 in Johnson et al. 1994), with a shape parameter of $\gamma$ and scale parameter $\beta = 1/(\lambda\alpha)^{1/\gamma}$.

Note that in the geometric model described above, $A(t)$ is quadratic in time (assuming the plume does not truncate), so $\gamma = 2$, but using the more flexible diffusion model, the scaling is with $\sqrt{t}$, giving the value of $\gamma = \frac{3}{2}$ in Eq. (12).

We need to estimate the Weibull scale parameter $\beta$ as it provides the means for estimating $\lambda$ from $\tau_1$ via Eq. (12). Irrespective of the shape parameter (so for any model of arrivals founded on the assumption of a Poisson distribution of fish in the environment), the maximum-likelihood estimator for $\beta$ is $\hat{\beta} = \tau_1$ (Johnson et al. 1994, p. 656), so the variance of the estimator is equal to the variance of the first arrival time, which is known from the properties of the Weibull distribution:

$$\mathbf{V}[\hat{\beta}] = \mathbf{V}[\tau_1] = \beta^2[\Gamma(1 + \frac{2}{\gamma})] \qquad (13)$$

where $\Gamma(z)$ is the Gamma function (a generalisation of the factorial).

We will now determine the precision of estimating fish abundance ($\lambda$) from first arrival times, irrespective of the precise model used for the arrival process.

Assuming $\alpha$ is known (i.e. the speeds of fish and current), we obtain an estimator for $\lambda$, using the definition of the scale parameter above:

$$\hat{\lambda} = \frac{1}{\alpha\hat{\beta}^\gamma} \qquad (14)$$

In this, $\hat{\beta}^\gamma$ is distributed as $\tau_1^\gamma$ which is an exponential distribution with mean $\beta$ (Johnson et al. 1994). $\alpha\hat{\lambda}$ must be distributed the same as $1/\beta^\gamma$, which is the reciprocal of an exponential distribution, the mean of which is $\beta$.

The exponential distribution is a special case of a Gamma distribution, having a shape parameter $a = 1$. A classic result is that if any variable $X$ follows a Gamma distribution with *any* shape parameter $a$, then its reciprocal $Y = 1/X$ follows an inverse Gamma distribution with shape parameter $a$. Unfortunately, it is also well known that the inverse Gamma distribution having shape parameter $a = 1$ has no finite expectation (implying that it cannot be predicted). Strictly, $\mathbf{E}[Y] < \infty$ if $a > 1$, so our case is right at the limit of expectations existing. Because $\mathbf{V}[Y] < \infty$, only if $a > 2$, the present problem is deep within the range having infinite variance, so no sample of $\tau_1$ can yield an estimate $\hat{\lambda}$ with non-zero certainty. In practice, the initial disturbing effect of the lander arriving on the bottom makes the assumption of Poisson arrivals invalid for a short time from the start, where an immediate visit from a fish is practically ruled out. This 'smoothes' the extreme conclusion of the statistical theory somewhat. Excepting the initial 'disturbance transient', the assumed Poisson distribution is readily justified as being the standard null model (minimum assumptions) for any random distribution in space. Thus, using well-known and long-established probability theory, we have shown that for a range of reasonable arrival models, assuming fish do not show social interactions and are not distracted from the bait, then the time of first arrival is a very poor predictor of their abundance.

## REGRESSION MODEL

**Using the rising phase of the time series.** Next we examine a regression on the rising phase of the time series to estimate arrival rate and thereby abundance.

For practical purposes, we define the rising phase as the region from $t = 0$ to the time of arrival of the fish causing the maximum number to be observed together (which we label as $\tau^{\star}$). The start of the time series is chosen because fish are potentially arriving from $t = 0$. The time when numbers reach maximum will not usually be the exact end of the rising phase, because the trend in expected numbers is superimposed with stochastic variation. However, since the distribution of the resulting error is approximately symmetric about the expected number-maximum, the observed maximum is close to an unbiased estimator.

The analysis assumes that observations are independent and that departure rate is zero during the rising phase ($\rho_d = 0$ in $t = 0, \tau^{\star}$) and that all fish attracted to the bait are seen; hence, arrivals are measured by $m_t = m(t)$ (see Fig. 1; error of these assumptions will underestimate abundance).

Non-linear regression, describing the model $m_t = \Lambda t^{\varphi}$, accommodates both the geometric cross-current forager (where $\Lambda = \lambda \alpha$ and $\varphi = 2$) and the diffusion approximation (where $\Lambda = \frac{vu}{v+u} 4\lambda \sqrt{D/\pi}$ and $\varphi = \frac{3}{2}$), but also permits a purely empirical estimate of $\Lambda$ and $\varphi$, for which we have no theoretical explanation (it may involve complicating factors such as turbulence of the plume). This empirical fit should be included to demonstrate the plausibility (or otherwise) of the theoretically justifiable options. Thus, we have 3 regression models to compare (linear in the parameter in the first 2 cases and non-linear in the last case), summarised below.

Model 1: $\mathbf{E}[m_t] = \Lambda t^2$ : linear geometry
Model 2: $\mathbf{E}[m_t] = \Lambda t^{3/2}$ : diffusion limit in fish behaviour
Model 3: $\mathbf{E}[m_t] = \Lambda t^{\varphi}$ : empirical model

**Regression predictions.** Here, we show the method in use on examplary data taken from observations of *Coryphaenoides armatus* in the Nazaré Canyon, west of Portugal (King 2006). Normal regression assumes that errors are approximately normally distributed with zero mean and equal variances. Inspection of the residuals (using residual and normal quantile plots, Fig. 4) for the examplary data does not support this assumption, especially as the variance can be seen increasing with fitted values.

Conversely, our theoretical models of arrival assume that $m_t$ is Poisson distributed—chosen as it is a neutral model (zero information) for the spatial distribution of fish. To test this, we transformed the data prior to regression. Assuming that $m_t$ follows a Poisson distribution with mean value $\lambda t^{\varphi}$, then $\sqrt{m_t} + \sqrt{(m_t + 1)}$ will approximate a normal distribution (especially for small values of $\lambda t^{\varphi}$, as here), with an approximate mean value of $2\sqrt{\lambda t^{\varphi}}$ and unit variance (Freeman & Tukey 1950).

The normal quantile plots on transformed data (Fig. 5) provide statistical justification for these Poisson assumptions. Fitting the transformed models gave the results provided in Table 2.

The fitting of these models to the data is shown in Fig. 6, which indicates that both Models 2 and 3 have been very successful, the deviance values (Table 2) confirm this. It is impossible to distinguish Models 2 and 3 in the fitting of plots, because the empirical fit for $\varphi$ (Model 3) gave an estimate very close to $\frac{3}{2}$, which

Table 2. Results from regression models, assuming $\sqrt{m_t} + \sqrt{m_t + 1}$ normally distributed around twice the square root of the estimated mean. Deviance is the residual sum of squares

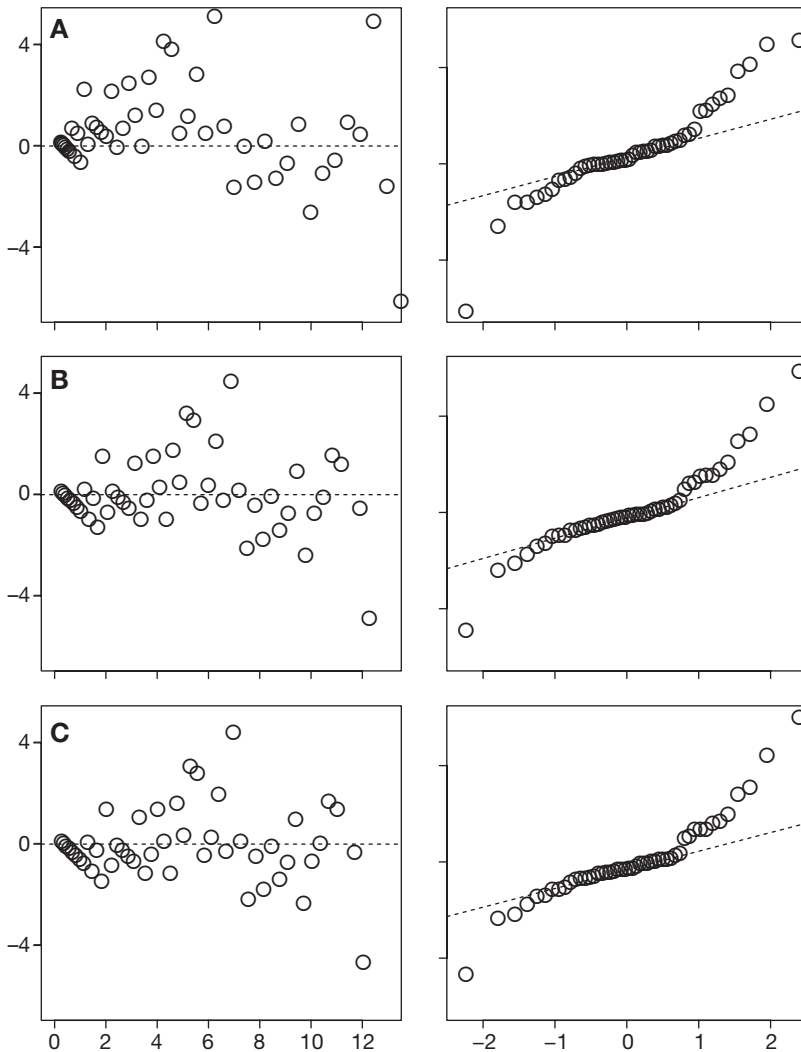|  | $2\sqrt{\hat{\Lambda}}$ | $SE(2\sqrt{\hat{\Lambda}})$ | $\hat{\varphi}$ | $SE(\hat{\varphi})$ | Deviance |
|---|---|---|---|---|---|
| Model 1 | 0.10577 | 0.00272 | – | – | 32.23 |
| Model 2 | 0.28474 | 0.00613 | – | – | 22.85 |
| Model 3 | 0.29025 | 0.06177 | 1.4902 | 0.1084 | 22.84 |

Fig. 4. Diagnostic plots of models for untransformed data. (A) Model 1, (B) Model 2 and (C) Model 3. Left column: residuals against fitted values for the 3 models. Right column: quantile plots (empirical quantiles of residuals against quantiles of the standard normal distribution), reference lines pass through the first and third quartiles

was the value assumed in Model 2. The residual plots (Fig. 5) support these conclusions, showing good compliance with the statistical assumptions. On this basis, we select Model 2 (the diffusive swimming fish), with transformation of Poisson distributed data, as the best model for the rising phase of the time series. Using the test data, we obtain a value for $\hat{\Lambda}$ of 0.02027 (95% confidence intervals: 0.01859 and 0.02202). This can be translated into a 95% confidence interval for $\lambda$ (the fish abundance) using a suitable estimate of $D$ in $\Lambda = \frac{vu}{v+u} 4\lambda\sqrt{D/\pi}$. The dependence on an unknown parameter $D$ is a nuisance, which we will see again in the next section. There is a clear need for estimating it from observations of the behaviour of relevant fish species.

This method is easy to implement: Models 1 and 2 are simply linear regressions. Model 3 is non-linear in the $\varphi$ parameter, adding a slight complication, but it is still simple to implement with standard statistical software.

## HIDDEN MARKOV MODEL

**Using the whole time series.** The maximum use of information theoretically yields the highest achievable precision. In this section we will show how the whole time series can be analysed, using a model of departures from the bait of fish both seen and unseen by the camera.

Referring to Fig. 1, we regard $n(t)$ as hidden and the $\rho$ and $\zeta$ terms as parameters that can be estimated using the statistical technique of a hidden Markov model (HMM) (Cappé et al. 2005)—now commonly used in automatic speech recognition. With this method, the system represented by Fig. 1 is assumed to be a 2-state Markov process $(m_t, n_t)$, with parameters estimated from $m_t$ (again, using the non-italic font to denote observed counts). The 'hidden state' is the number of fish at the bait, but outside the camera view $(n_t)$.

We make the simplifying assumption that fish move among visible and hidden states between camera shots, so the observed $m_t$ at each time step is a sample from a binomial distribution with number parameter $x_t = n_t + m_t$ and some constant probability parameter $p$. This $p$ corresponds to the visible fraction of the fish at the bait.

Since the diffusive model of arrivals (Eq. 9) was the best supported by regression in the previous section, it is chosen to represent arrivals here, so we assume $\rho_a(\lambda,t) = \tilde{\rho}_a\sqrt{t}$ (note tilde notation for empirically estimated parameters). We aim to estimate the prefactor $\tilde{\rho}_a$, to derive from it a fish abundance estimate $\tilde{\lambda}$ using Eq. (9).

Now a model for departures is needed. The mean flux away from the bait zone at time $t$ is proportional to the number of fish present at $t$. To take account of the behaviour of fish towards a depleting bait, we define the departure rate $\rho_d$ as follows. The probability of any fish leaving in a short time interval $t$ to $t + h$ is set to $\rho_d h$ (approximated to first order in $h$), which we assume to be a linear function of time. However, we continue
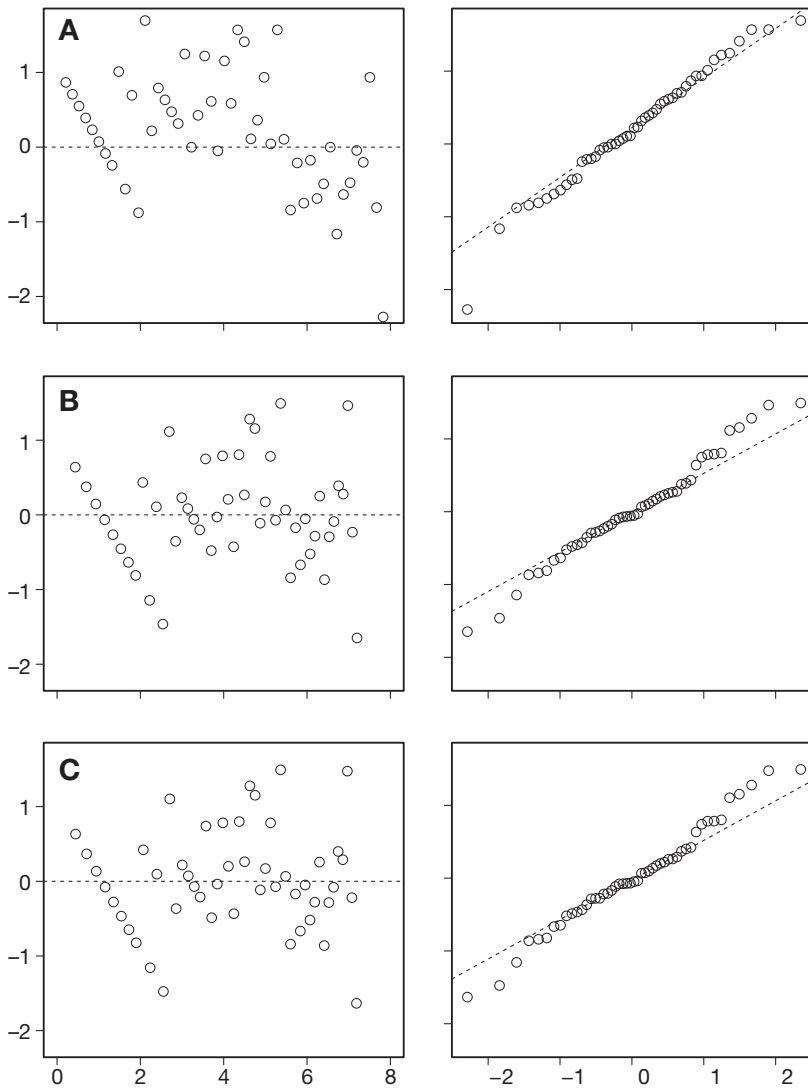
Fig. 5. Diagnostic plots of models for transformed data, assuming a Poisson arrival process. (A to C) Panels as in Fig. 4

(This moment method is probably very close to a maximum-likelihood estimate, and reduces computational complexity significantly). We then tabulate the fit, i.e. the profile likelihood, for each combination of $\tilde{z}$ and $\tilde{p}$. The parameter estimate is then chosen as that parameter combination which results in the largest profile likelihood, i.e. we tune the estimator to optimise predictions of the number of fish in view at the next image frame. Further details are given in Appendix 1.

**Predictions.** Fig. 7 shows the negative log-likelihood (often shortened to likelihood) of parameters $z$ and $\rho_d$. The optimal estimate, defining the minimum of this function, is at $\hat{z} = 0.0011$ min$^{-2}$ and $\hat{p} = 0.33$. An approximate 95% confidence region is given by parameter values for which the likelihood does not exceed the minimum value by $>2q$, where $q$ is the 95% quantile in a chi-squared distribution with the number of degrees of freedom equal to the number of estimated parameters. In the figure, this region is inside the $l = 455$ contour line.

Note that this predicts about one-third of the fish present in the bait zone are visible to the camera. The predicted value of $z$ in this case, means that a fish in the bait zone at peak numbers time $\tau^\star$ will stay for at least 34 further minutes with 50% probability (found from solving $\exp[-\int_0^T \rho_d(t)dt] = 0.5$). Fish that arrive later will tend to stay a shorter time, since the departure rate grows with time.

Fig. 8 shows the profile likelihood for the prefactor in fish arrival rate. We see that the maximum-likelihood estimate is 0.061 min$^{-3/2}$, with a 95% confidence interval between 0.044 and 0.091. From this we can find the number of fish having arrived in the bait region at time $t$: $N_t = \int_0^T 0.061\sqrt{t}\,dt = 0.041 t^{3/2}$ ($t$ in minutes). Using the estimate $\tilde{p}$, this predicts that $0.013 t^{3/2}$ fish will be visible to the camera (as long as they have not begun leaving, i.e. for $t < \tau^\star$). This is close to half the prediction made by the regression method in the previous section (there, Model 2 gave $2\sqrt{\Lambda} = 0.284$, so $0.02 t^{3/2}$ fish would be present), but that had assumed the visible fraction $p = 1$.

Using the parameter estimates gives a model of predicted numbers of fish in the bait zone ($m_t + n_t$), the output if which is shown in Fig. 9, together with the observed number of fish. This result demonstrates the potential for the camera to underestimate numbers, a

with the assumption that no fish depart before the time of the peak in observed fish numbers ($\tau^\star$), so we have $\tilde{\rho}_d = \max(0, \tilde{z}[t - \tau^\star])$, where the slope $\tilde{z}$ estimates a new and unknown parameter representing the rate at which the bait loses its attractiveness with time. Note that this model was chosen to be parsimonious and appropriate in the example case used, but others could be substituted (it is only necessary to specify $\tilde{\rho}_d$ as a function of time).

**Estimations.** We need to estimate 3 parameters: the arrival rate prefactor $\tilde{\rho}_a$ (from which we can find $\tilde{\lambda}$), the departure rate $\tilde{\rho}_d$, represented by $\tilde{z}$ and the visible fraction $\tilde{p}$.

The process requires a first 'guess' at a value of $\tilde{z}$ and $\tilde{p}$. For this, we choose $\tilde{\rho}_a$, so that the total expected number of observed fish matches the actual count.
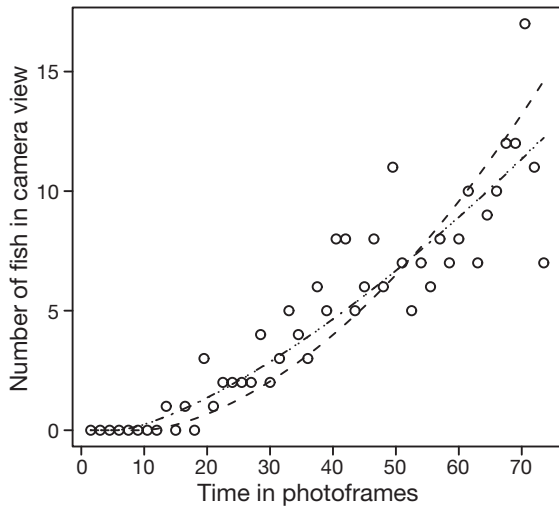
Fig. 6. Regression models. Circles: observed data; dashed line: Model 1; dotted line: Model 2; dot-dashed line: Model 3—all using transformed data. Note that Models 2 and 3 are indistinguishable at the scale plotted



Fig. 8. Profile negative log-likelihood for estimating the arrival rate prefactor $\tilde{\rho}_a$. The 95% confidence interval is indicated where the curve crosses the dashed line

phenomenon now empirically confirmed by Jamieson et al. (2006) (though with a different lander to that used in generating the test data). Some may be surprised at the closeness with which the HMM model follows the data. The explanation is that the HMM is not a simple 3-parameter model (as often encountered in basic statistics), but a Markov model, which at each time step uses the whole time series along with the 3 parameters in a constantly updating calculation of expected numbers in the next photoframe. The fact that it follows the data consistently suggests that the parameter estimates are good.
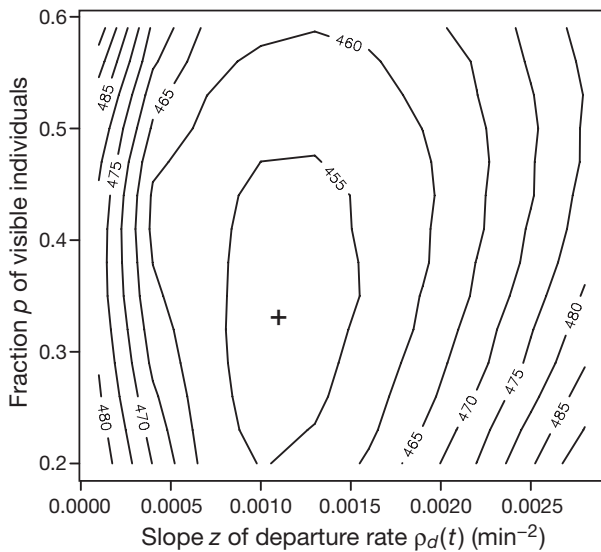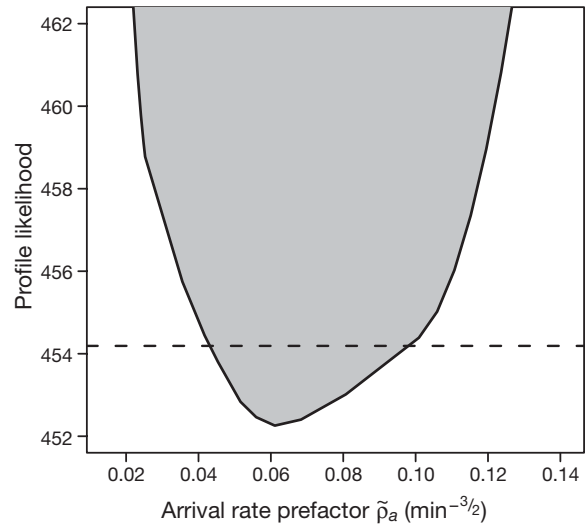


Fig. 7. Contour plot of the negative log-likelihood function for estimating departure rate slope $z$ and observable fraction $p$

## DISCUSSION

Having examined 3 different methods for estimating abundance from fish counts at a bait, we are in a position to make recommendations for studies with cross-current foraging fish in reasonably stable currents. The first of these may be very surprising for biologists who have relied on first arrival times for their estimates. This measure was found to have a theoretically infinite variance and, in practice, to make a very poor estimator, as long as we can assume that fish do not socially interact, or become distracted from the bait. This finding is independent of the specific model of fish arrivals used, as it is a consequence of assuming a random distribution of fish in the environment. The weakness of first arrival time as a predictor had been obscured by the use of deterministic models, which did not allow uncertainty to be quantified. Despite several reports of correlations between $\tau_1$ and independently measured abundance (e.g. Sainte-Marie & Hargrave 1987), there is no support from statistical theory for using first arrival times.

Conversely, a regression on the rising phase of the time series (the period until maximum numbers are expected), assuming Poisson distribution of residuals and a diffusive scaling of arrival rate, gave a precise measure of abundance with the test data. This method is theoretically sound and simple to use, so we recommend it for circumstances where its assumptions are found to hold. These assumptions are specifically that fish behave independently, are distributed at random in the environment, and that all fish arriving at the bait are seen upon arrival. Further, that fish do not leave
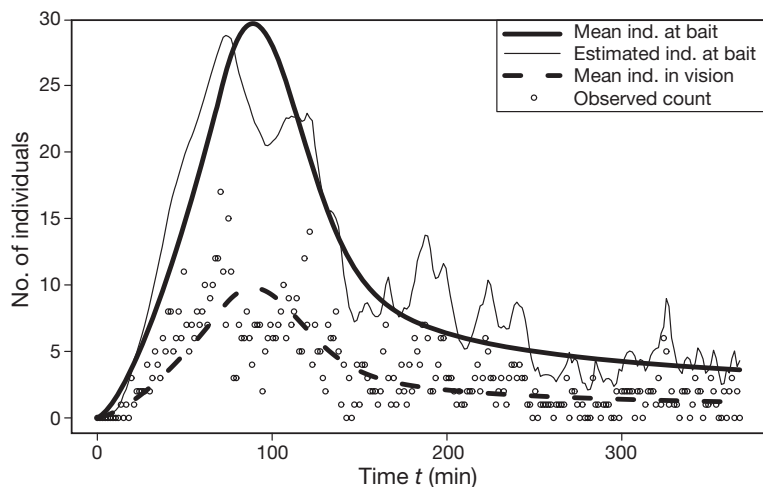
Fig. 9. Examplary data (counted individuals in each photo) with hidden Markov model (HMM)-fitted estimates. HMM with full knowledge of observations (———); model based on parameter estimates with the mean of observed count (━━━); model of observed (visible) fish only, based on mean observed count (▬ ▬)

the bait until after maximum numbers are observed, that the plume does not change greatly in direction during the rising phase, and that the usual assumptions for regression hold.

The more flexible method of HMM is recommended for its smaller set of assumptions, though it incurs a cost in complexity and additional parameters to be estimated. The assumptions of the HMM method are that fish are distributed randomly in the environment, act independently (including at the bait) and that the plume does not change greatly in direction during the time series (though the method could be adapted to cope with violations of the latter 2 assumptions). We wish to emphasise that it is very important to determine if the assumptions of any method are met prior to use.

In our example, for models of both the regression and HMM methods, we introduced a new parameter $D$, defined as fish searching diffusivity. Estimates of $D$ should be sought if this simple and flexible model is to be used. $D$ has the form of swimming speed squared, divided by the frequency of changing direction whilst searching for plumes: $D = w^2/\mu$. Search speeds ($w$) are often known, but new effort is needed to estimate turning frequencies ($\mu$) from observations of fish behaviour. Abundance estimates are sensitive to $\sqrt{D}$, which is much less than their sensitivity to swimming speed, so, given a reasonable estimate of a fish's turning frequency $\mu$, a working estimate of $D$ is attainable. It is possible to interpret $D$ more broadly as an empirical parameter that depends in part on non-linear extension of the plume, non-ideal swimming strategies of the fish and other factors that 'spoil' the theoretical ideals of the geometric model. However, a calibration

based on independent abundance estimates (e.g. from trawls) would be necessary to estimate $D$, following this interpretation.

The regression and, in our example (though not necessarily or generally), the HMM method assumed that departure rate from the bait is zero until the maximum number of fish is seen ($\tau^*$). Strictly, this is not likely, partly because of randomness in fish behaviour and partly because the maximum should appear when the departure rate exceeds the arrival rate, which by definition is greater than zero. The resulting bias underestimates abundance in the regression method. It is therefore very important to ensure that this assumption is a reasonable approximation (i.e. that the maximum occurs at a time after deployment that is less than the expected staying time of a fish). The HMM method is less affected by this bias from the rising phase, because the iterative fitting can compensate using the remainder of the time series. If there is a long rising phase, we recommend the HMM method with some simple departure model designed to reflect the researchers' beliefs about departures. In other words, the HMM method should be customised to the particular case for which it is to be used.

Practical application of the regression method is simple, using most statistical software packages. Time acts as the independent variable in a univariate non-linear regression for number of fish observed in each camera exposure (as in the described Model 2). The intercept should be set as zero (no fish at time zero), leaving the slope to be estimated, giving $\Lambda$ (as in Model 2), which enables $\lambda$ to be found from the various velocity estimates. We illustrated diagnostic plots to check that the assumptions of this method support its use; we especially recommend residual and quantile plots for this. Practical use of the HMM method requires some programming, for example, in a statistical or mathematics package—details are provided in the Appendix.

The problem caused by fish attracted to the apparatus, but not photographed on the bait (Collins et al. 1999) is well known and has been demonstrated by Jamieson et al. (2006, admittedly using a design of lander that is not usual for abundance estimation). The HMM method estimates the size of the resulting bias simultaneously while estimating arrival and departure rates. In the example shown, the HMM method estimated an arrival rate close to half that of the regression method when using the same model of arrivals over the same section of the time series. Independent measures of the 'hidden fraction' of fish would be hard to obtain, unless cameras were set to observe the lander system.

The HMM method requires a model of departures as well as arrivals. Priede & Merrett (1998) fitted an empirical curve to the estimated staying time (which determines departure rate) using the time of maximum number of fish ($\tau^*$) minus the first arrival time ($\tau_1$), thus assuming staying time to be constant. However, bait depletion and scavenger competition mitigate against this assumption, especially for long time series. In principle, we could understand both effects in terms of optimal foraging theory, as suggested by Priede & Merrett (1998), who showed that staying time (as they defined it) declined with fish abundance (independently determined with trawls). However, using the marginal value theorem (Charnov 1976), suggested by this result, requires a model for competition and satiation, leading to considerable complications and introducing new parameters. For the present purpose, we suggest the parsimonious, single-parameter model in which the probability of departing in a small time interval increases at a constant rate with elapsed time. The gradual increase in departure probability that we hypothesise is most likely related to bait depletion, which can be estimated from the photographs. This could set limits (at least) on the $z$ parameter of $\rho_d$, so even crude estimates of bait depletion rate could be useful in using the HMM model. Clearly, there are opportunities to improve on this, but each development of sophistication needs to be justified by quantity and quality of data available.

Broadening the discussion, our overall model of fish behaviour can be extended in a number of ways to address specific biological issues. For example, species that show either gregarious or food-swarming behaviour could be represented by alternative statistical models of dispersion (the Poisson model being a null-hypothesis), and allowing for autocorrelation in the time series in the regression technique could probably accommodate most of these effects. Territoriality can be taken into account by truncating the arrival rate after a time representing territory size, and this approach can also be used to allow for rival attractants (e.g. natural food falls) in the environment. Changes in current velocity over measurement time are often observed in the deep sea and are almost inevitable (due to tides) in shallower seas. The result is a more complicated plume shape and perhaps changes in fish swimming velocities. To take account of this, our model could be treated as a piecewise fit to the number of observed fish, using different current parameters over different sections. More sophisticated modelling of the plume will allow a more precise description of how arrival rate depends on abundance, but not necessarily more precise abundance estimates, since additional parameters reduce statistical power. As stated earlier, it is possible to include plume spreading in the diffusivity parameter $D$ of fish searching behaviour.

LITERATURE CITED

Bailey D, Priede I (2002) Predicting fish behaviour in response to abyssal food falls. Mar Biol 141:831–840

Cappé O, Moulines E, Rydén T (2005) Inference in hidden Markov models. Springer-Verlag, Heidelberg

Charnov E (1976) Optimal foraging: the marginal value theorem. Theor Popul Biol 9:129–136

Collins M, Yau C, Nolan C, Bagley P, Priede I (1999) Behavioural observations on the scavenging fauna of the Patagonian slope. J Mar Biol Assoc UK 79:963–970

Collins M, Yau C, Guilfoyle F, Bagley P, Everson I, Priede I, Agnew D (2002) Assessment of stone crab (Lithodidae) density on the South Georgia slope using baited video cameras. ICES J Mar Sci 59:370–379

Dusenbery D (1989) Optimal search direction for an animal flying or swimming in a wind or current. J Chem Ecol 15:2511–2519

Freeman M, Tukey J (1950) Transformations related to the angular and the square root. Ann Math Stat 21:607–611

Henriques C, Priede I, Bagley P (2002) Baited camera observations of deep-sea demersal fishes of the Northeast Atlantic Ocean at 15–28° N off West Africa. Mar Biol 141:307–314

Jamieson A, Bailey D, Wagner H, Bagley P, Priede I (2006) Behavioural responses to structures on the seafloor by the deep-sea fish *Coryphaenoides armatus*: implications for the use of baited landers. Deep-Sea Res I 53:1157–1166

Johnson N, Kotz S, Balakrishnan N (1994) Continuous univariate distributions, Vol 1, 2nd edn. Wiley-Interscience, New York

King N (2006) Deep-sea ichthyofauna of contrasting locations: mid-Atlantic Ridge, Nazare Canyon (North Atlantic Ocean) and Crozet Plateau (Southern Indian Ocean), with special reference to the abyssal grenadier, *Coryphaenoides* (*Nematonurus*) *armatus* (Hector, 1875). PhD dissertation, University of Aberdeen

Lapointe V, Sainte-Marie B (1992) Currents, predators, and the aggregation of the gastropod *Buccinum undatum* around bait. Mar Ecol Prog Ser 85:245–257

Lokkeborg S, Olla B, Pearson W, Davis M (1995) Behavioral responses of sablefish, *Anoplopoma fimbria*, to bait odor. J Fish Biol 46:142–155

Okubo A (1980) Diffusion and ecological problems: mathematical models. Springer-Verlag, Heidelburg

Priede I, Bagley P (2000) *In situ* studies on deep-sea demersal fishes using autonomous unmanned lander platforms. Oceanogr Mar Biol Annu Rev 38:357–392

Priede I, Merrett N (1996) Community studies. 2. Estimation of abundance of abyssal demersal fishes: a comparison of data from trawls and baited cameras. J Fish Biol Suppl A 49:207–216

Priede I, Merrett N (1998) The relationship between numbers of fish attracted to baited cameras and population density: studies on demersal grenadiers *Coryphaenoides* (*Nematonurus*) *armatus* in the abyssal NE Atlantic Ocean. Fish Res 36:133–137

Priede I, Smith K, Armstrong J (1990) Foraging behavior of abyssal grenadier fish—inferences from acoustic tagging and tracking in the North Pacific Ocean. Deep-Sea Res 37:81–101

Priede I, Bagley P, Armstrong J, Smith K, Merrett N (1991) Direct measurement of active dispersal of food-falls by deep-sea demersal fishes. Nature 351:647–649

Priede I, Bagley P, Smith A, Creasey S, Merrett N (1994) Scavenging deep demersal fishes of the Porcupine Seabight, Northeast Atlantic—observations by baited camera, trap and trawl. J Mar Biol Assoc UK 74:481–498

Sainte-Marie B, Hargrave B (1987) Estimation of scavenger abundance and distance of attraction to bait. Mar Biol 94:431–443

Vabo R, Huse G, Ferno A, Jorgensen T, Lokkeborg S, Skaret G (2004) Simulating search behaviour of fish towards bait. ICES J Mar Sci 61:1224–1232

Webster D, Weissburg M (2001) Chemosensory guidance cues in a turbulent chemical odor plume. Limnol Oceanogr 46:1034–1047

Yau C, Collins M, Bagley P, Everson I, Nolan C, Priede I (2001) Estimating the abundance of Patagonian toothfish *Dissostichus eleginoides* using baited cameras: a preliminary study. Fish Res 51:403–412

Yen J, Weissburg M, Doall M (1998) The fluid physics of signal perception by mate-tracking copepods. Philos Trans R Soc B 353:787–804

Zimmer-Faust R, Finelli C, Pentcheff N, Wethey D (1995) Odor plumes and animal navigation in turbulent waterflow—a field study. Biol Bull (Woods Hole) 188:111–116

**Appendix 1.** Implementing the HMM technique

The hidden Markov model (HMM) method is implemented through an HMM filter. In the following, we briefly describe how this filter is constructed, so that those familiar with modelling can replicate the technique. In-depth treatments of the theory of HMMs are found in Cappé et al. (2005). The filter first aims to estimate the total number of fish, $x_t = n_t + m_t$, in which $x_t$ is a stochastic variable that may take integer values between 0 and a sufficiently large bound $K$ on the total number of fish at the bait.

The filter needs the transition probabilities of $x_t$. Assume that $x_t = i$ and consider $x_{t+h}$, where $h$ is a fixed short time interval. If a fish has arrived, then $x_{t+h} = i + 1$; the probability of this is $g_{i(i+1)}(t) = h \times \rho_a(t)$. If a fish has departed, then $x_{t+h} = i - 1$; the probability of this is $g_{i(i-1)}(t) = i \times h \times \rho_d(t)$. Alternatively, nothing has happened; the probability of this is $g_{ii}(t) = 1 - g_{i(i-1)}(t) - g_{i(i+1)}(t)$. These are valid approximations when $h$ is small compared to $\rho_a(t)$, $\rho_d(t)$ and the rate of change of these functions. Typical camera sampling times of 30 to 120 s (in our example it was $h = 90$ s) will give sufficient resolution in most practical cases.

The predictive filter consists of $\Phi(t)$, a (row) vector, the $i$th entry $\Phi_i(t)$ of which is the probability that $x_t = i$, given all observations strictly prior to $t$. Similarly, the row vector $\psi(t)$ has entries $\psi_i(t)$ being the probability that $x_t = i$, given all observations no later than $t$. The 'data update' transforms $\Phi(t)$ to $\psi(t)$ by taking the observation $m_t = \mathsf{m}_t$ into account:

$$\psi_i(t) = \frac{\Phi_i(t)}{l(t)} \mathbf{P}\{m_t = \mathsf{m}_t \mid x_t = i\} \qquad (A1)$$

Here, $l(t) = \Sigma_i \mathbf{P}\{m_t = \mathsf{m}_t | x_t = i\}$ is a normalization ensuring that $\Sigma_i \psi_i(t) = 1$. These probabilities are computed using the assumption that, conditional on $x_t = i$, $m_t$ is binomially distributed with number parameter $i$ and probability parameter $p$:

$$\mathbf{P}\{m_t = \mathsf{m}_t \mid x_t = i\} = \binom{i}{\mathsf{m}_t} p^{\mathsf{m}_t}(1-p)^{i-\mathsf{m}_t} \qquad (A2)$$

The time update projects $\psi(t)$ forward in time to obtain a prediction $\Phi(t+h)$:

$$\Phi_j(t+h) = \sum_{i=j-1}^{j+1} \psi_i(t) g_{ij}(t) \qquad (A3)$$

The time update and the data update are iterated forwards in time; the initial condition is $\psi_0(0) = 1$ and $\psi_i(0) = 0$ for $i \neq 0$. At the end of the iteration, we evaluate the likelihood function $L(\tilde{z}, \tilde{p}) = \prod_t l(t)$. Recall that $\tilde{\rho}_a$ is estimated by a moment method rather than with the likelihood method. The likelihood function is optimized numerically. For estimated parameters, we 'smooth' to obtain probability vectors $\pi(t)$, with $\pi_i(t)$ denoting the probability that $x_t = i$, given all observations. This smoothing is an iteration backwards in time:

$$\pi_i(t) = \psi_i(t) \sum_{j=i-1}^{i+1} g_{ij}(t) \frac{\pi_j(t+h)}{\Phi_j(t+h)} \qquad (A4)$$

with terminal condition $\pi(T) = \psi(T)$.